BPB Reports

Regular Article

Calcineurin Binds to a Unique C-Terminal Region of NBCe1-C, the Brain Isoform of NBCe1 and Enhances its Surface Expression

Naomi Hasegawa,[a] Naoya Hatano,[b] Suguru Tohyama,[a] Sayaka Kita,[a] Katsuhiko Mikoshiba,[c] and Akihiro Mizutani*[,a]

[a]*Department of Pharmacotherapeutics, Showa Pharmaceutical University, Machida, Tokyo 194–8543, Japan;* [b]*Division of Applied Cell Biology, Graduate School of Interdisciplinary Science and Engineering in Health Systems, Okayama University, Okayama 700–8530, Japan;* [c]*Laboratory for Developmental Neurobiology, Brain Science Center, RIKEN, Wako, Saitama 351–0198, Japan*

Received February 13, 2019; Accepted February 13, 2019

NBCe1 (electrogenic Na^+/HCO_3^- cotransporter 1) is a product of gene *SLC4A4* and has five splice variants, NBCe1-A through NBCe1-E. In agreement with an essential role of NBCe1 in cellular pH regulation, human families carrying missense mutations of gene *SLC4A4* show proximal renal tubular acidosis. Some of them exhibit brain function-related symptoms, such as migraine and mental retardation, but physiological roles of NBCe1 in brain function remain unclear. To gain insights into NBCe1-specific functions in the brain, we herein identified proteins that specifically bind to a unique C-terminal region of NBCe1-C, a brain-specific NBCe1 isoform. We found that a catalytic subunit of calcineurin binds to the C terminus of NBCe1-C in the mouse cerebellum. Heterologous-coexpression experiments revealed that calcineurin binds to NBCe1-C via a "PQIRIE" motif at its C terminus. The interaction enhanced cell surface expression of NBCe1-C, resulting in an increase of its transporter activity, for which the phosphatase activity of calcineurin was essential. When NBCe1-C was stably expressed in HeLa cells, its cell surface expression was enhanced by an intracellular Ca^{2+} concentration increase and was suppressed by FK506, a specific inhibitor of calcineurin. These mechanisms of surface expression and transport activity of NBCe1-C regulated by the Ca^{2+}–calcineurin axis indicate specialized functions of NBCe1-C in the brain.

Key words NBCe1, calcineurin, astrocytic pH regulation, synaptic cleft

INTRODUCTION

Electrogenic Na^+/HCO_3^- cotransporter 1 (NBCe1) is a product of the *SLC4A4* gene and has five splice variants (NBCe1-A through -E) in humans and mice.[1–3] Tissue expression of proteins NBCe1-A, -B, and -C has already been well characterized. The NBCe1-A protein is highly expressed in renal proximal tubules where NBCe1-A reabsorbs HCO_3^- and plays a critical role in the maintenance of normal systemic pH. The NBCe1-B protein is more widely expressed, i.e., in the pancreas, cornea, ileum, heart, and brain, and the NBCe1-C protein is predominantly expressed in the brain. NBCe1-B and NBCe1-C share the same N-terminal segment encoded by exon 2, and their transport activities are increased by the binding of IRBIT to this segment.[4–6] NBCe1-C has a unique C-terminal cytoplasmic tail produced by skipping of exon 24.[7] Protein expression of NBCe1-D and -E transcripts has not been reported.[8]

Igarashi *et al*. have originally reported two unrelated patients who presented with proximal renal tubular acidosis (pRTA) and carried causative homozygous missense mutations in the *SLC4A4* gene.[9] To date, 17 pRTA patients carrying several types of mutations in the *SLC4A4* gene have been reported.[10,11] Slc4A4-deficient mice that lack the functional expression of NBCe1 also show severe pRTA and die before weaning,[8,12] suggesting that in kidneys, NBCe1-A plays an essential part in the maintenance of systemic pH. Patients with pRTA caused by *SLC4A4* mutations often present with extrarenal manifestations including ocular aberrations such as glaucoma and cataract, stunted growth, mental retardation, calcification in brain basal ganglia, migraine, and enamel deficiency. Although some of these problems are secondary to systemic acidosis caused by NBCe1-A deficiency, considering the widespread tissue expression of NBCe1-B and -C, these isoforms can be involved in the extrarenal manifestations.

In the brain and other organs, the regulation and homeostasis of both intra- and extracellular pH (pHi/pHo) are crucial. In particular, neural activities depend on continuous synaptic transmission that causes rapid changes in pHi/pHo of the synapses. Because the activities of many ion channels that participate in synaptic transmission are sensitive to pH changes, various acid/base transporters that are expressed at the plasma membrane of not only neurons but also astrocytes are essential for the maintenance of proper pHi/pHo. NBCe1-C is expressed mainly in astrocytes[13,14] but is expressed in neuron to a much lesser extent.[15,16] In astrocytes, NBCe1-C is localized at the plasma membrane of astrocytes that surround neurons,[13] this arrangement allows astrocytes to respond to synaptic transmission through depolarization-induced alkalinization, a well-known phenomenon attributed to astrocytic NBCe1.[17] More recently, astrocytic NBCe1 was shown to be involved in

*To whom correspondence should be addressed. e-mail: mizutani@ac.shoyaku.ac.jp

a metabolic crosstalk between neurons and astrocytes.[18] The C-terminal cytoplasmic tail shared by NBCe1-A and NBCe1-B is critical for their membrane expression.[19] Nonetheless, the functional properties of the unique C-terminal tail of NBCe1-C, particularly regarding the involvement in the distribution in perisynaptic processes of astrocytes, have not been elucidated.

In this study, to gain insights into NBCe1-C functions in the brain, we focused on the unique C-terminal cytoplasmic tail and tried to isolate proteins that bind to this region. We found that a catalytic subunit of calcineurin, a calcium/calmodulin-dependent protein phosphatase, binds to the C-terminal tail through the canonical binding motif PQIRIE and enhances membrane expression of NBCe1-C.

MATERIALS AND METHODS

All the experiments in this study were approved by the Institutional Animal Care and Use Committee of Showa Pharmaceutical University and were conducted in accordance with the Guidelines for Proper Conduct of Animal Experiments (Science Council of Japan, 2006). All biochemical experiments were conducted at 2–4°C.

A GST Pull-Down Assay A GST fusion protein containing the C-terminal region of NBCe1-C (GST-NBCe1-C/Ct) was expressed in *Escherichia coli* and purified as described previously.[20] A whole adult murine brain was homogenized in homogenization buffer (0.32 M sucrose, 10 mM 4-(2-hydroxyethyl)-1-piperazineethanesulfonic acid [HEPES]-NaOH [pH 7.5], 25 mM NaF, and the Protease Inhibitor Cocktail EDTA free [Nacalai Tesque]), and the homogenate was centrifuged at 1,000 × *g* for 15 min. A clear whole-brain lysate was prepared by the addition of SDS (final concentration 0.1%) to the supernatant, followed by centrifugation at 100,000 × *g* for 45 min at 4°C. The lysate was incubated with GST-NBCe1-C/Ct or GST (control) for 4 h, and the proteins that bind to each GST fusion protein were captured by Glutathione Sepharose 4B beads (GE Healthcare). After the beads were washed five times with a buffer consisting of 20 mM HEPES-NaOH (pH 7.5), 100 mM NaCl, 25 mM NaF, and 0.2% Triton X-100, the bound proteins were examined by SDS-PAGE.

Immunoprecipitation and Western Blotting For immunoprecipitation from the cerebellum, an adult mouse cerebellum was homogenized as described above, and the homogenate was centrifuged at 100,000 × *g* for 45 min. The precipitate was resuspended in 1 mL of homogenization buffer containing 0.2% Triton X-100 followed by centrifugation at 100,000 × *g* for 45 min. The supernatant was incubated with 1.5 µg of an anti-CaNAα antibody (Santa Cruz Biotechnology, cat. # D-9) or 1.5 µg of control mouse IgG for 1 h. Immune complexes were collected by incubation with protein G Sepharose beads (GE Healthcare) for 4 h. After washing of the beads with lysis buffer, each immunoprecipitate was analyzed by western blotting.

For immunoprecipitation from HEK293T cells, the cells were transiently transfected with various combinations of expression plasmids using TransIT 2020 Reagent (Mirus Bio). At 48 h after transfection, the cells were washed with PBS and solubilized with cell lysis buffer (20 mM HEPES-NaOH [pH 7.5], 100 mM NaCl, 25 mM NaF, 0.2% Triton X-100, and the Protease Inhibitor Cocktail EDTA free). After centrifugation at 12,000 × *g* for 20 min, the resulting supernatants were incubated with anti-FLAG-beads (Anti-FLAG®M2 Affinity Gel, Sigma-Aldrich) or anti-HA–magnetic beads (Pierce anti-HA Magnetic Beads, Thermo Scientific, cat. # 88836) for 4 h. After a wash of the beads with cell lysis buffer, each immunoprecipitate was analyzed by western blotting. The antibodies used for detection are an anti–human SLC4A4 rabbit polyclonal antibody (1/1,000 dilution, Proteintech, cat. # 11885-1-AP), an anti–PP2B-Aα mouse monoclonal antibody (1/1,000, Santa Cruz Biotechnology, cat. # D-9), an anti-HA rat monoclonal antibody (1/1,000, Roche, cat. # 3F10), and an anti-FLAG mouse monoclonal antibody (1/1,000, Wako, cat. # 1E6). For detection of NBCe1-C, a specific anti–NBCe1-C rabbit polyclonal antibody was prepared as follows. The purified GST fusion protein carrying the C terminus of NBCe1-C (see above) was subcutaneously injected into a rabbit four times at 2-week intervals, and an anti–NBCe1-C antibody was affinity-purified from antisera by means of an MBP fusion protein (carrying the same region), which was covalently linked to Sepharose beads (CNBr-activated Sepharose, GE Healthcare). Specificity of the antibody is shown in Supplementary Fig. S1. Western blotting was carried out basically as described previously.[20] To visualize the immune complexes, horseradish peroxidase (HRP)-conjugated secondary antibodies (1/4,000, GE healthcare) and chemiluminescent reagent Luminata Forte Western HRP Substrate were employed. Chemiluminescent signals were digitized via an ImageQuant LAS 4000 mini system (GE Healthcare) and analyzed by the ImageJ software.

Mass Spectrometry Analysis Liquid chromatography with tandem mass spectrometry (LC-MS/MS) analysis was carried out as described previously.[21] MS/MS data were acquired in a data-dependent mode by the LCMS solution software (Shimadzu) and were converted to a single text file (containing *m*/*z* of the observed precursor peptide, fragment ion *m*/*z*, and intensity values) by Mascot Distiller (Matrix Science). The file was analyzed with the Mascot (Matrix Science) MS/MS Ion Search to assign the obtained peptides to entries of the SwissProt database. For protein identification, the criteria were as follows: (i) Mascot scores above the statistical significance threshold ($p < 0.05$) and (ii) at least one top-ranked unique peptide matching the identified protein.

Cell Surface Expression Assay

1) Immunofluorescence-based analysis (a sequential staining strategy)

HeLa cells maintained in DMEM supplemented with 10% of fetal calf serum were transiently transfected with various constructs using TransIT 2020 Reagent (Mirus Bio). At 24 h after transfection, the cells were replated on a 12 mm glass coverslip precoated with poly-l-lysine (100 µg/mL, Sigma-Aldrich, cat. # P9155) and cultured for another 24 h. The cells were fixed with 4% paraformaldehyde (PFA) in PBS for 15 min. After blockage with 2% normal goat serum (NGS, Wako) in PBS, the cells were first incubated with the anti-HA rat monoclonal antibody for 3 h at room temperature to detect cell surface NBCe1. After a thorough wash with PBS, the cells were permeabilized with 0.1% Triton X-100 in PBS for 5 min and then blocked with 2% NGS in PBS. To detect total NBCe1, the cells were then incubated with the rabbit anti-SLC4A4 polyclonal antibody for 2 h at room temperature. Cell surface and total NBCe1 were visualized with secondary antibodies: an Alexa Fluor 594-conjugated anti-rat IgG antibody (Thermo Fisher, cat. # A11007) and an Alexa Fluor 488-conjugated anti-rabbit IgG antibody (Thermo Fisher, cat. # A11034),

respectively. Each fluorescence signal was acquired from the maximum intensity projection images obtained from 20 sections of Z-series covering each cell from top to bottom as captured by confocal microscopy system A1R (Nikon Instruments) and was analyzed in the NIS Element software (Nikon Instruments).

2) Alkaline phosphatase (ALP)-based analysis

HeLa cells stably expressing extracellularly HA-tagged wild-type NBCe1-C were selected with 1 mg/mL G418 (Nacalai Tesque). Parental and NBCe1-C-expressing HeLa cells were seeded in a 96-well plate and incubated in DMEM supplemented with 10% of fetal calf serum for 24 h. The cells were next treated with a vehicle (0.1% dimethyl sulfoxide; DMSO) or 2 μM 4-bromo A23187 (Abcam) in the growth medium in the absence or presence of 10 μM FK506 (Cayman Chemical) for 4 h at 37°C and 5% CO_2. For detection of surface NBCe1-C, the cells were fixed with 4% PFA followed by blocking with 2% NGS in PBS. After that, the cells were incubated with the anti–HA-tag antibody for 3 h at room temperature. After extensive washing, the cells were incubated with the rabbit anti-rat IgG polyclonal antibody conjugated with ALP (1/10,000, Sigma-Aldrich, cat. # A6066) for 1 h. The amounts of NBCe1 on the cell surface were quantified by measuring ALP activity with *p*-nitrophenyl phosphate as a substrate (Bio-Rad, cat. # 1721063) and by monitoring the elevation of absorbance (405 nm) on Varioskan Flash (Thermo Scientific) after initiation of the enzymatic reaction. For detection of total NBCe1-C expression levels, a 0.1% Triton X-100 permeabilization step was added after fixation with PFA, and the other procedures were the same as those for surface expression detection. Background absorbance was measured in parent HeLa cells and was subtracted from each absorbance value of cells subjected to various treatments at various time points. The resulting net absorbance was analyzed, and the elevation of the value during 9 min from the start was defined as ALP activity representing the amounts of surface or total NBCe1-C.

pHi Measurements pHi was measured by recording SNARF-1 fluorescence intensities at emission wavelengths 580 and 640 nm with excitation at 488 nm by means of a confocal microscope (A1R, Nikon Instruments). During the measurement, perfusion solutions were kept at 37°C. HeLa cells were transfected with one of the IRES-AcGFP/NBCe1 constructs with or without constitutively active (CA-) or phosphatase-dead (PD-) truncation mutant of CaNAα/CaNB. Preliminary experiments showed that over 80% of GFP-positive cells coexpressed CaNAα. At 48 h after transfection, the cells were loaded with 20 μM SNARF-1 in normal buffer (140 mM NaCl, 5 mM KCl, 1 mM $MgCl_2$, 1 mM $CaCl_2$, 10 mM glucose, 10 mM HEPES-NaOH [pH 7.4]) for 30 min at 37°C in a humidified atmosphere containing 5% of CO_2. For stabilization, the cells were perfused with normal buffer for 10 min, and pHi measurement was started from the last 1 min of normal-buffer perfusion. The cells were then perfused with Na^+-free buffer called $Na^+(-)$ (115 mM NMDG-Cl, 5 mM KCl, 1 mM $MgCl_2$, 1 mM $CaCl_2$, 10 mM glucose, 2.5 mM HEPES, and 25 mM tetraethylammonium bicarbonate) for 2 min, and transport activity of NBCe1 was induced by changing the buffer to Na^+-containing buffer called $Na^+(+)$ (115 mM NaCl, 5 mM KCl, 1 mM $MgCl_2$, 1 mM $CaCl_2$, 10 mM glucose, 2.5 mM HEPES, 25 mM $NaHCO_3$) with perfusion for 2 min. Finally, the buffer was replaced with $Na^+(-)$ buffer, and perfusion was kept for 2 min. Na^+/H^+ exchanger activities were blocked by 10 μM *S*-(*N*-ethyl-*N*-isopropyl) amiloride (EIPA; Sigma) during perfusion with a buffer containing HCO_3^-. pHi was represented by the SNARF-1 fluorescence ratio (640 nm/580 nm), and the pHi change was the difference between the fluorescence ratios at each time point and the average value of the fluorescence ratio during the stabilizing phase (the last 1 min of incubation with normal buffer).

Determination of the Phosphorylation Level of NBCe1-C The phosphorylation level of NBCe1-C was determined as reported previously.[22] Briefly, after preincubation with a phosphate-free medium, HEK293T cells transfected with HA-tagged NBCe1-C or a deletion mutant of NBCe1-C lacking the PQIRIE motif (Δ_{CN}NBCe1-C) with CA-CaNAα/CaNB were metabolically labeled with [^{32}P]orthophosphate (0.8 mCi/mL) (Perkin Elmer). After incubation for 4 h at 37°C in a humidified atmosphere containing 5% of CO_2, NBCe1 was immunoprecipitated with the anti-HA antibody, and its radioactivity was quantified on a BAS500 bioimaging analyzer (Fuji Photo Film).

Statistical Analyses All these analyses were performed in EZR (Saitama Medical Center, Jichi Medical University, Saitama, Japan), which is a graphical user interface for R.[23] In the data presented in Figs. 3–5, outliers were excluded by the Smirnov–Grubbs test, and normality of the distribution was verified by the Kolmogorov–Smirnov test. In Figs. 3 and 4, we carried out Kruskal–Wallis and *post hoc* Steel-Dwass tests. In Figs. 5 and 7, we performed one-way analysis of variance (ANOVA) and the *post hoc* Tukey HSD test. For all analyses, the level of statistical significance was set to $p < 0.05$. All box whiskers were created in Excel 2016.

RESULTS

A Catalytic Subunit of Calcineurin Was Isolated from the Mouse Cerebellum as an NBCe1-C–Binding Protein Of all five alternative splicing variants of NBCe1, NBCe1-C has a unique C-terminal cytoplasmic tail that is generated by alternative splicing.[1,24] We produced a GST fusion protein containing this unique region (Fig. 1A, in *red*) and tried to isolate the proteins that specifically bind to this region from mouse brain extracts. Next, the bound proteins were analyzed by SDS-PAGE, and a protein band with a molecular mass of ~59 kDa was detected (Fig. 1B, an arrow). LC-MS/MS analysis of peptides resulting from trypsin digestion of the band identified catalytic subunits of calcineurin α and β as its major components (Table 1). All other proteins were PDZ domain proteins (Table 1); this result is understandable because the C terminus contains a PDZ-ligand motif, ETTL.[1,3,7] Subsequently, we focused on the NBCe1-C–calcineurin interaction because of their highest Mascot scores (Table 1). First, to confirm the interaction in an intact cellular context, HA-tagged NBCe1-C, a FLAG-tagged catalytic subunit of calcineurin α (CaNAα), and the regulatory subunit of calcineurin (CaNB) were coexpressed in HEK293T cells, and CaNAα was immunoprecipitated. We found that HA-tagged NBCe1-C was coimmunoprecipitated with FLAG-tagged CaNAα (Fig. 1C). We then also tried to detect a possible interaction between NBCe1-C and calcineurin *in vivo*. One report has shown higher expression of CaNAα compared to CaNAβ in the cerebellum,[25] and CaNAα mRNA is highly expressed in astrocytes according to an RNA sequence transcriptome database[14] (http://web.stanford.edu/group/barres_lab/brain_rnaseq.html). Given that NBCe1-C

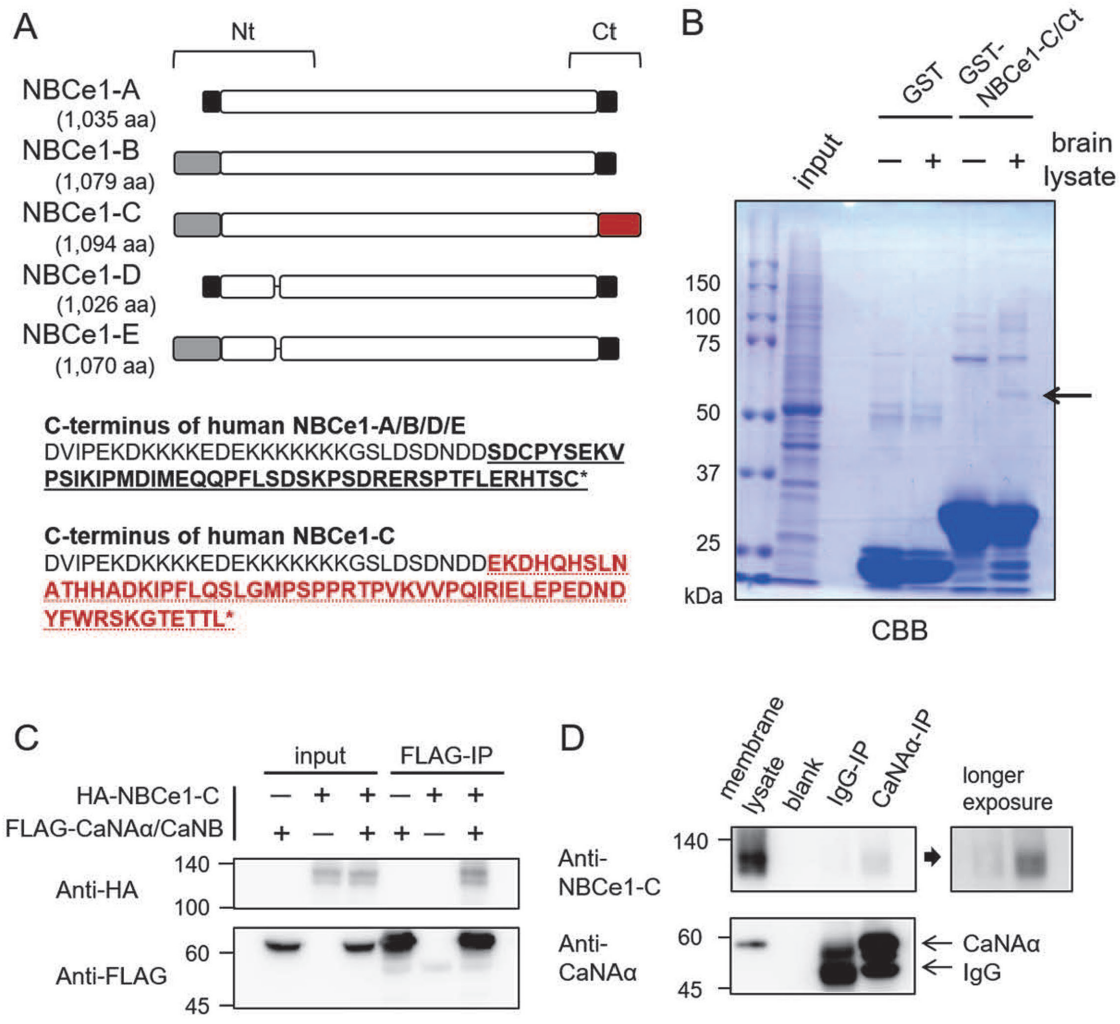

Fig. 1. CaNA Was Isolated from the Mouse Cerebellum as an NBCe1-C–Binding Protein

(A) Schematic representation of the protein structure of five splice variants of NBCe1, and amino acid sequence of the C-terminal region of NBCe1. The unique sequence of NBCe1-C is highlighted in red. **(B)** Bound proteins obtained by the GST pull-down assay using GST-NBCe1-C/Ct were visualized with Coomassie Brilliant Blue (CBB) staining. An arrow indicates a ~59 kDa band that was identified as calcineurin Aα (CaNAα) and calcineurin Aβ by LC-MS/MS analysis. **(C)** Interaction between HA-NBCe1-C and FLAG-CaNAα in transfected HEK293T cells was verified by coimmunoprecipitation with the anti-FLAG antibody. The upper panel shows amounts of HA-tagged NBCe1-C in input samples (left 3 lanes) and in coimmunoprecipitated fractions (right 3 lanes). A lower panel presents amounts of FLAG-CaNAα in input samples (left 3 lanes) and in immunoprecipitated fractions (right 3 lanes). **(D)** A complex between NBCe1-C and CaNAα in mouse cerebellar membrane fractions was revealed by coimmunoprecipitation with the anti-calcineurin Aα antibody. The upper left panel indicates each amount of NBCe1-C in a lysate of a cerebellar membrane fraction (left 2 lanes) and in coimmunoprecipitated fractions (right 2 lanes). The upper right panel presents a longer-exposure image of coimmunoprecipitated fractions. The lower panel shows each amount of CaNAα in the cerebellar membrane fraction (left 2 lanes) and in immunoprecipitated fractions (right 2 lanes).

Table 1. Mouse Brain Proteins that Bind to a Unique C-Terminal Region of NBCe1-C

Swiss Prot ID	Protein Name	Molecular weights (Da)	Mascot score
P2BB_MOUSE	Catalytic subunit of calcineurin beta isoform	59,163	576
PP2BA_MOUSE	Catalytic subunit of calcineurin alpha isoform	58,606	571
MPP6_MOUSE	MAGUK p55 subfamily member 6	62,592	83
GOPC_MOUSE	Golgi-associated PDZ and coiled-coil motif-containing protein	50,631	74
SNTA1_MOUSE	Alpha-1-syntrophin	53,632	59
MPP2_MOUSE	MAGUK p55 subfamily member 2	61,517	46
SNX27_MOUSE	Sorting nexin-27	60,950	35

also manifests higher expression in the cerebellum and astrocytes,[13] we focused on the interaction between CaNAα and NBCe1-C. Immunoprecipitates from the 0.2% Triton X-100–solubilized mouse cerebellar membrane fraction with the anti-CaNAα antibody contained significant amounts of NBCe1-C as revealed by NBCe1-C isoform-specific immunoblotting (Fig. 1D). This finding indicated that NBCe1-C forms a complex with CaNAα *in vivo*.

Calcineurin Binds to NBCe1-C via a Calcineurin-Docking Motif in the C-Terminal Region of NBCe1-C It is well known that calcineurin recognizes most of its substrates via two distinct classes of docking motifs, PxIxIT and LxVP.[26–28] We searched the sequence of the C terminus of NBCe1-C and found the "PQIRIE" motif, which fits the consensus sequence

and is present only in the C-terminal tail of NBCe1-C (not NBCe1-A/B/D/E; Fig. 1A). Sequence alignment of NBCe1-C orthologs suggested that this PQIRIE motif is well conserved among animal species (Fig. 2A). To confirm that this motif is essential for the binding of NBCe1-C to CaNAα, we created a deletion mutant of NBCe1-C lacking the PQIRIE motif (Fig. 2A, Δ_{CN}NBCe1-C) and examined the binding of CaNAα to Δ_{CN}NBCe1-C and to NBCe1-B. A coimmunoprecipitation assay revealed that neither NBCe1-B nor Δ_{CN}NBCe1-C bound to CaNAα (Fig. 2B), suggesting that CaNAα bound to NBCe1-C via the PQIRIE motif in the C-terminal tail. CaNAα is a Ca^{2+}/CaM-dependent Ser/Thr protein phosphatase. Thus, our next question was whether the phosphatase activity is required for the binding. We examined the binding of NBCe1-C to a constitutively active (CA-) or phosphatase-dead (PD-) truncation mutant of CaNAα by a coimmunoprecipitation assay. We found that NBCe1-C constantly bound to both CA- and PD-mutants as well as to wild-type CaNAα (Fig. 2B), indicating that the phosphatase activity of CaNAα was not required for its binding to NBCe1-C.

Calcineurin Enhances the Surface Expression of NBCe1-C To understand the physiological significance of CaNA binding to NBCe1-C, we transiently expressed NBCe1-C, Δ_{CN}NBCe1-C, or NBCe1-B in HeLa cells and examined their subcellular distribution. Both NBCe1-B and NBCe1-C were distributed throughout the cell, whereas Δ_{CN}NBCe1-C accumulated around the nucleus (Fig. 3A). Next, we evaluated cell surface expression of NBCe1-B, NBCe1-C, or Δ_{CN}NBCe1-C by a sequential staining protocol involving extracellular HA-tag staining first, followed by common NBCe1 epitope staining (see *Materials and Methods*); the levels of NBCe1-B and NBCe1-C were comparable and were significantly higher than that of Δ_{CN}NBCe1-C (Fig. 3B). This finding suggested that CaNAα binding could affect surface expression of NBCe1-C, and we examined the effects of coexpression of CA- or PD-CaNAα on surface expression of NBCe1-C, NBCe1-B, or Δ_{CN}NBCe1-B. Coexpression of CA-CaNAα significantly enhanced surface expression of all NBCe1 protein versions. Nonetheless, the extent of upregulation of NBCe1-C (1.9-fold, $p < 0.001$) was much higher than that of NBCe1-B (1.2-fold, $p < 0.05$) or Δ_{CN}NBCe1-C (1.3-fold, $p < 0.05$; Fig. 4A and B). Furthermore, PD-CaNA was capable of binding to NBCe1-C but did not enhance surface expression of NBCe1-B, NBCe1-C, or Δ_{CN}NBCe1-C (Fig. 4A and B). These findings indicated that surface expression of NBCe1-C was specifically enhanced by CaNAα and that the enhancement required CaNAα binding as well as its phosphatase activity.

Calcineurin Enhances the Transport Activity of NBCe1-C The finding of enhancement of NBCe1-C surface expression by calcineurin raises a possibility that the transport activity of

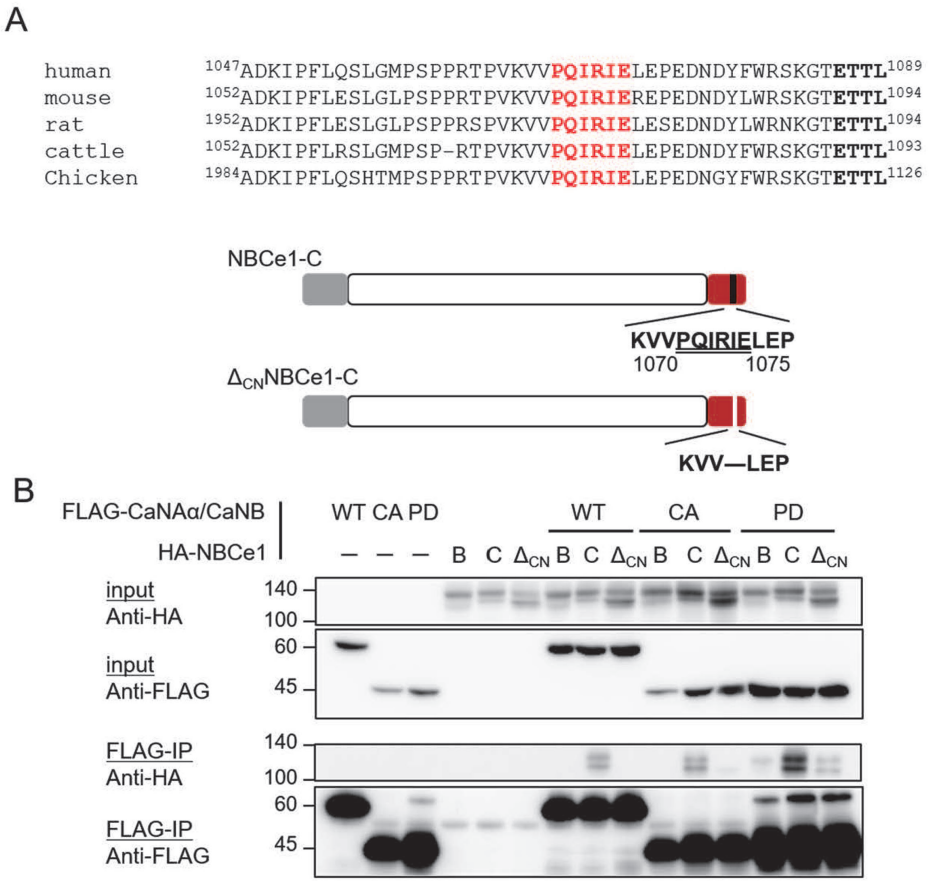

Fig. 2. Calcineurin Binds to NBCe1-C via a Calcineurin-Docking Motif

(A) *Top*: Alignment of C-terminal regions of NBCe1-C from various animal species shows that the PQIRIE motif (in red) is conserved. Each amino acid sequence is from GenBank [accession numbers NM_001134742.1 (humans), NM_001136260.1 (mice), XM_006250791.3 (rats), XM_015471675.2 (cattle), and XM_025150084.1 (chicken)]. *Bottom*: Schematic representation of the protein structure and sequences of Δ_{CN}NBCe1-C, a mutant of NBCe1-C devoid of the PQIRIE motif. **(B)** CaNAα specifically bound to NBCe1-C (C) but neither to NBCe1-B (B) nor Δ_{CN}NBCe1-C (Δ_{CN}), for which phosphatase activity of CaNAα was not required. Each NBCe1 construct was coexpressed with the wild type full-length CaNAα (WT), constitutively active (CA)-CaNAα, or phosphatase-dead (PD)-CaNAα. The two upper panels present expression of each NBCe1 construct (top) and each CaNAα construct (bottom), revealed with the anti-HA antibody and anti-FLAG antibody, respectively. The lower two panels show each coimmunoprecipitated NBCe1 with CaNAα (upper panel) and each immunoprecipitated CaNAα (lower panel) as revealed by means of the anti-HA antibody and anti-FLAG antibody, respectively.

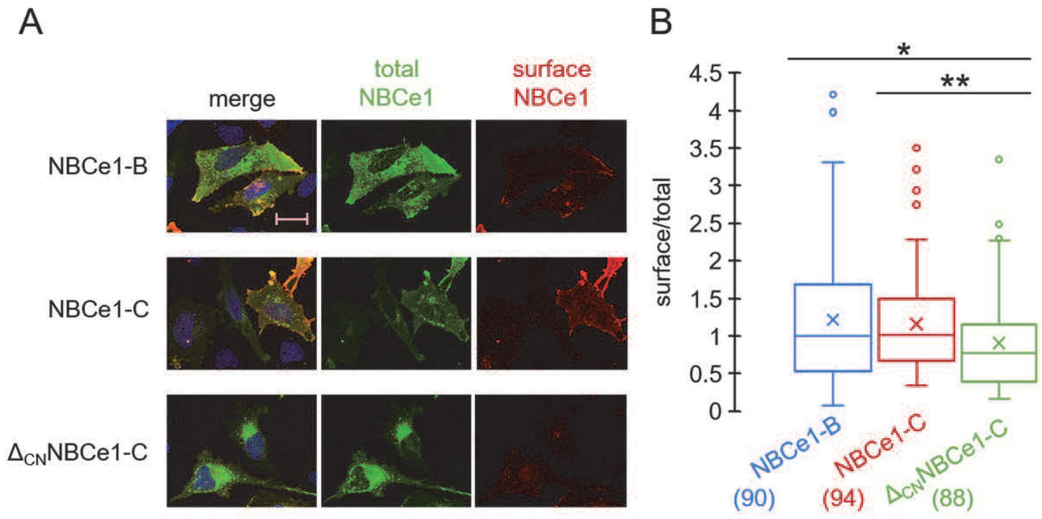

Fig. 3. Subcellular Distribution of Heterologously Expressed NBCe1-B, NBCe1-C, or NBCe1-C Lacking the Calcineurin-Docking Motif in HeLa Cells

(A) One of the NBCe1 constructs was transiently expressed in HeLa cells, and its surface expression and subcellular distribution was visualized with sequential staining. NBCe1 on the cell surface was visualized with the extracellular HA-tag antibody (red), and total NBCe1 was visualized with the anti-SLC4A4 antibody (green). Upper panels: NBCe1-B, middle panels: NBCe1-C, lower panels: Δ_{CN}NBCe1-C lacking the calcineurin-docking motif. A scale bar is 25 μm. **(B)** Surface expression was determined by the fluorescence intensity ratio of membrane signals to total signals. Cells were collected from three independent experiments (sample numbers are in the parentheses). Relative surface expression levels of NBCe1-B, NBCe1-C, and Δ_{CN}NBCe1-C were calculated using a median value of NBCe1-B set to 1.0. Kruskal–Wallis test, $p = 0.0046$ and Steel–Dwass *post hoc* test, * and ** represent $p < 0.05$ and $p < 0.01$, respectively.

NBCe1-C could be regulated by calcineurin. Thus, we examined the effects of coexpression of CA- or PD-CaNAα on the transport activity of NBCe1-C or Δ_{CN}NBCe1-C by measuring intracellular pH (pHi) elevation induced by Na^+-driven HCO_3^- transport, which was observed when the buffer was changed from Na^+(–) to Na^+(+) (Fig. 5A). In control HeLa cells, hardly any pHi changes induced by Na^+(+) buffer were observed in the presence of EIPA, an inhibitor of Na^+/H^+ exchangers, which also contribute to the pHi change in this experimental paradigm (Fig. 5A, vector, Na^+(+)). Meanwhile significant pHi elevation was observed in HeLa cells expressing NBCe1-C or Δ_{CN}NBCe1-C (Fig. 5A), indicating that the transport activity of expressed NBCe1 was properly assayed and was represented by velocity of the pHi elevation during initial 22 s after the change of the buffer from Na^+(–) to Na^+(+). Transport activity of NBCe1-C was higher (though not significantly; $p = 0.059$) than that of Δ_{CN}NBCe1-C (NBCe1-C:0.020 Δratio/s vs Δ_{CN}NBCe1-C:0.018 Δratio/s). CA-CaNAα coexpression significantly enhanced the activity of NBCe1-C (1.15-fold, $p < 0.05$) but did not affect that of Δ_{CN}NBCe1-C (1.06-fold, $p = 0.88$). In contrast, PD-CaNAα coexpression did not enhance NBCe1-C transport activity but rather reduced it (a 0.78-fold reduction as compared to CA-CaNA, $p < 0.001$; Fig. 5B). Given that the total expression levels of NBCe1 constructs were not affected by coexpression of either CaNAα construct (Fig. 2B), calcineurin enhanced cell surface expression of NBCe1-C and thereby its transport activity.

IRBIT is known as an activator protein for NBCe1-B/C. Because multisite phosphorylation of IRBIT is necessary for its binding to and activation of NBCe1-B/C,[4,29,30] CA-CaNAα coexpression could alter phosphorylation of IRBIT and its binding affinity for NBCe1-C. Accordingly, we tested whether CA-CaNAα coexpression could influence the binding of IRBIT to NBCe1-C or Δ_{CN}NBCe1-C. Immunoprecipitation of IRBIT revealed that coexpression of CA-CaNAα did not have any influence on the interaction between IRBIT and NBCe1-C or Δ_{CN}NBCe1-C (Fig. 6A). Therefore, the effects of calcineurin on surface expression/transport activity of NBCe1-C may be attributable to altered phosphorylation states of NBCe1-C rather than to those of IRBIT. Indeed, phosphorylation of NBCe1-C was apparently reduced by coexpression of CA-CaNAα, whereas phosphorylation of NBCe1-B or Δ_{CN}NBCe1-C was unchanged (Fig. 6B). NBCe1-C might be recognized by calcineurin via the PQIRIE docking motif and then dephosphorylated; therefore, surface expression of NBCe1-C may be regulated by a phosphorylation/dephosphorylation switch.

Surface Expression of NBCe1-C Is Enhanced in Response to Cytosolic Ca^{2+} Increase We demonstrated that surface expression and transport activity of NBCe1-C were enhanced by coexpression of CA-CaNAα. To examine the relevance of these findings in a more physiological context, we tested whether surface expression of NBCe1-C increases in response to elevation of intracellular Ca^{2+} concentration, which is a physiological stimulatory signal for calcineurin. We created a HeLa cell line stably expressing extracellularly HA-tagged NBCe1-C and determined the surface expression level when the influx of Ca^{2+} was induced by treatment with Ca^{2+} ionophore A23187 in the presence or absence of FK506, a specific inhibitor of calcineurin. Because the expression of NBCe1-C was too low to detect by immunofluorescence staining, the surface expression level was determined in the extracellular HA-tag–based immunoassay using the anti-HA antibody conjugated with ALP. When the cells were treated with A23187, surface expression of NBCe1-C significantly increased (1.31-fold, $p < 0.05$; Fig. 7A), and this enhancement was attenuated by FK506. Meanwhile, total NBCe1-C protein expression levels were comparable among the three groups (Fig. 7B). These data suggested that the surface amount of NBCe1-C stably expressed in HeLa cells was elevated by cytoplasmic Ca^{2+} concentration increase and subsequent calcineurin activation.

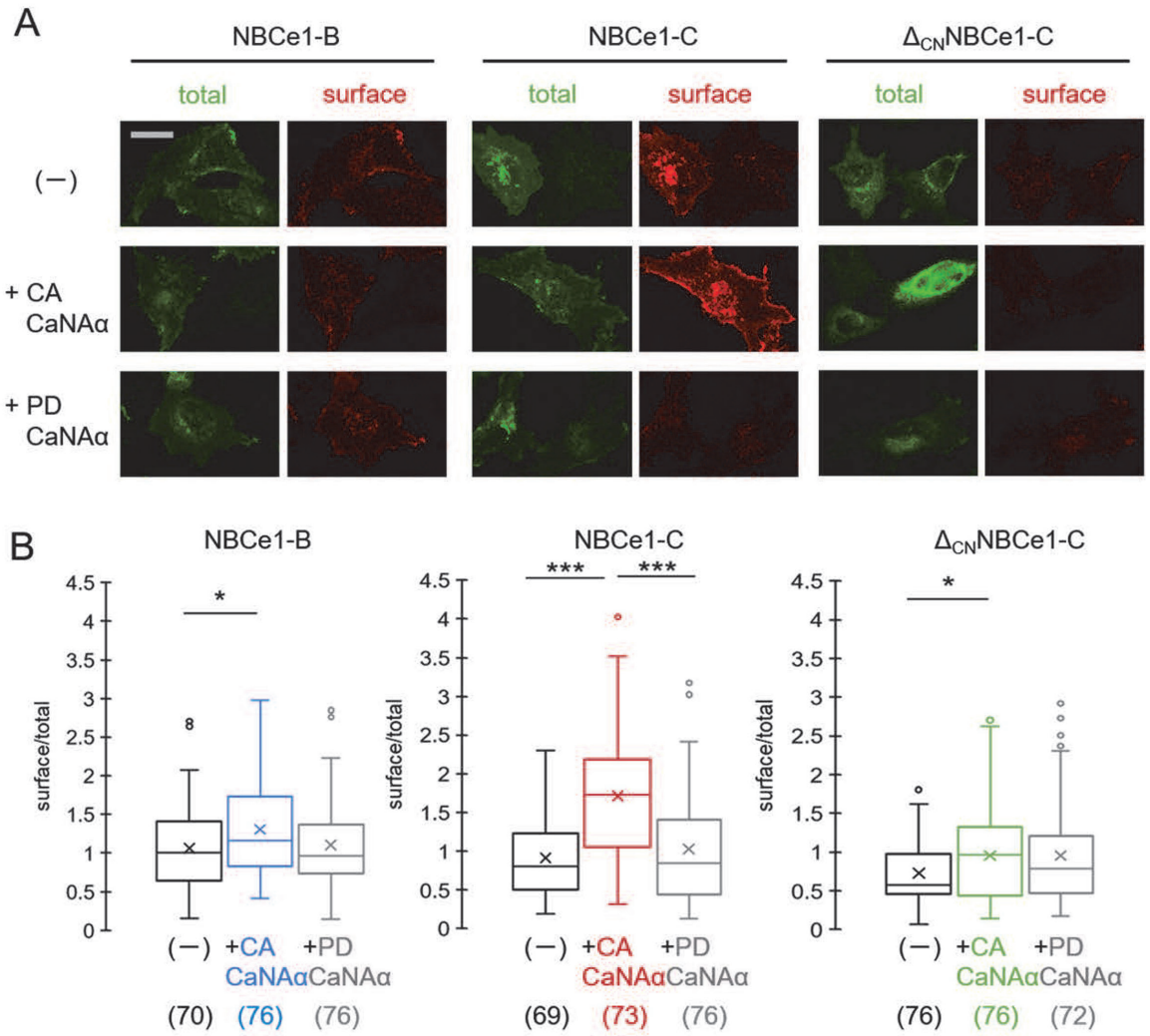

Fig. 4. Calcineurin Enhances Surface Expression of NBCe1-C

(A) Effects of co-expression of each CaNAα construct on surface expression level of each NBCe1 construct were examined in HeLa cells. NBCe1 on cell surface and total NBCe1 cellular distribution was examined as in Fig. 3. A scale bar is 25 μm. **(B)** Surface expression levels of each NBCe1 were determined as in Fig. 3. Cells were collected from three independent experiments (sample numbers in parentheses). Kruskal–Wallis test, NBCe1-B: $p = 0.03$, NBCe1-C: $p = 1.43*e^{-10}$, Δ_{CN}NBCe1-C: $p = 0.04$, and Steel–Dwass *post hoc* test, * and *** represent $p < 0.05$ and $p < 0.001$, respectively.

DISCUSSION

In this study, we demonstrated that a catalytic subunit of calcineurin binds to NBCe1-C via the PQIRIE motif present at the unique C terminus of NBCe1-C. Calcineurin enhanced the surface expression of NBCe1-C and increased the transporter activity, for which the phosphatase activity of calcineurin was found to be required; indeed, NBCe1-C was dephosphorylated by calcineurin. The regulation of NBCe1-C functions by the Ca^{2+}–calcineurin axis implies a specific function of NBCe1-C in the brain where rapid and local regulation of pH homeostasis is essential.

Some reports have shown that NBCe1-A and NBCe1-B, which are expressed in renal proximal tubular cells and pancreatic ductal cells, respectively, are localized to the basolateral plasma membrane.[31–34] According to the results of clinical and experimental studies on NBCe1-A/B mutants, cytoplasmic regions of both the N terminus and C terminus of NBCe1-A or -B are required for its proper targeting to the basolateral plasma membrane.[19,35,36] As for the C-terminal region of NBCe1-A/B, a 54-amino acid deletion at the C-terminal end of NBCe1-A/B and a 50-amino acid deletion at the C-terminal end of NBCe1-A impaired the plasma membrane targeting, whereas a shorter 26-amino acid deletion in NBCe1-A preserved the plasma membrane targeting but eliminated polarized targeting to the basolateral sites.[19,35] These results suggest that the C-terminal region contains both basolateral targeting and plasma membrane targeting signals. Li *et al*. have identified the "QQPFLS" sequence at the C terminus of NBCe1-A/B as a basolateral targeting signal.[35] In contrast to the epithelial cells, astrocytes and neurons in the brain have much more complex morphology. Although some molecular mechanisms for polarized targeting of transmembrane proteins are shared between epithelial cells and neural cells,[37] discrete molecular and structural mechanisms may exist, especially in neurons.[38,39] NBCe1-C has a unique C-terminal sequence lacking the QQPFLS motif but containing the "ETTL" PDZ ligand motif. Given that PDZ domain-based protein–protein interactions could serve as a platform for organization of cellular signaling,[40,41] the C-terminal tail of NBCe1-C may function as a specialized module regulating proper localization in neurons and astrocytes. Indeed, five PDZ domain proteins correspond-

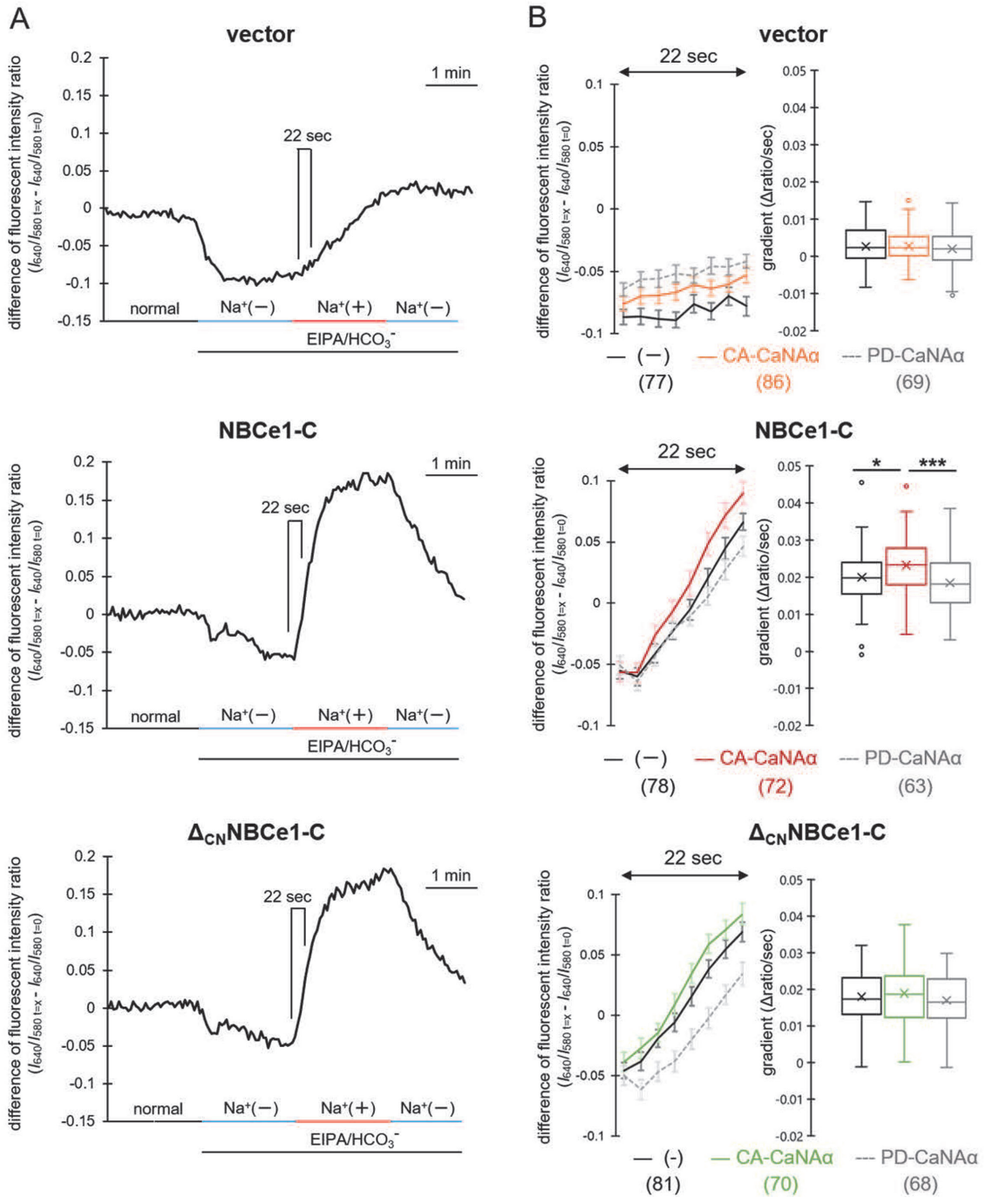

Fig. 5. Calcineurin Enhances the Transport Activity of NBCe1-C

(A) Transport activity of each NBCe1 construct expressed in HeLa cells was analyzed. pHi changes were displayed as a fluctuation of pH indicator SNARF-1 fluorescence intensity ratio (a difference in fluorescent intensity ratios). The lower part of the lines presents the composition of perfusion buffer. Transport activity of NBCe1 was expressed as intracellular alkalization induced by changing perfusion buffer from Na^+(–) to Na^+(+). During 22 s after the change of the buffer, an increase in speed in *Δ*fluorescence ratios stayed linear. Consequently, transport activity is represented by the gradient during this initial period. EIPA: *S*-(*N*-ethyl-*N*-isopropyl) amiloride. **(B)**. Effects of coexpression of each CaNAα construct on transport activity of each NBCe1 version were examined. Left-hand plots are zoomed-in images from the initial 22 s segment of plots in Fig. 5A. The right-hand box plot illustrates transport activity (gradient) of each NBCe1 construct coexpressed with each CaNAα construct. The cells were collected after five independent experiments (sample numbers are in parentheses). Error bars represent SEM. One-way ANOVA (vector: F = 0.46, $p = 0.63$; NBCe1-C: F = 7.22, $p < 0.001$; Δ_{CN}NBCe1-C: F = 1.13, $p = 0.32$) and the Tukey HSD *post hoc* test were conducted. * and *** represent $p < 0.05$ and $p < 0.001$, respectively.

ing to the molecular mass were isolated (Table 1). These are candidate molecules for regulating the surface expression and/or proper localization of NBCe1-C; unfortunately, the recovery amounts were too low for further analyses.

Both α and β catalytic subunits of calcineurin (CaNAα and CaNAβ) were isolated as proteins binding to the C-terminal tail of NBCe1-C, and the two had comparable Mascot scores (Table 1). We examined NBCe1-C binding to either CaNAα or CaNAβ in heterologous expression assays and immunoprecipitation experiments and noted comparable NBCe1-C binding to CaNAα and CaNAβ (see Supplementary Fig. S2). Furthermore, because the interaction between NBCe1-C and CaNAα

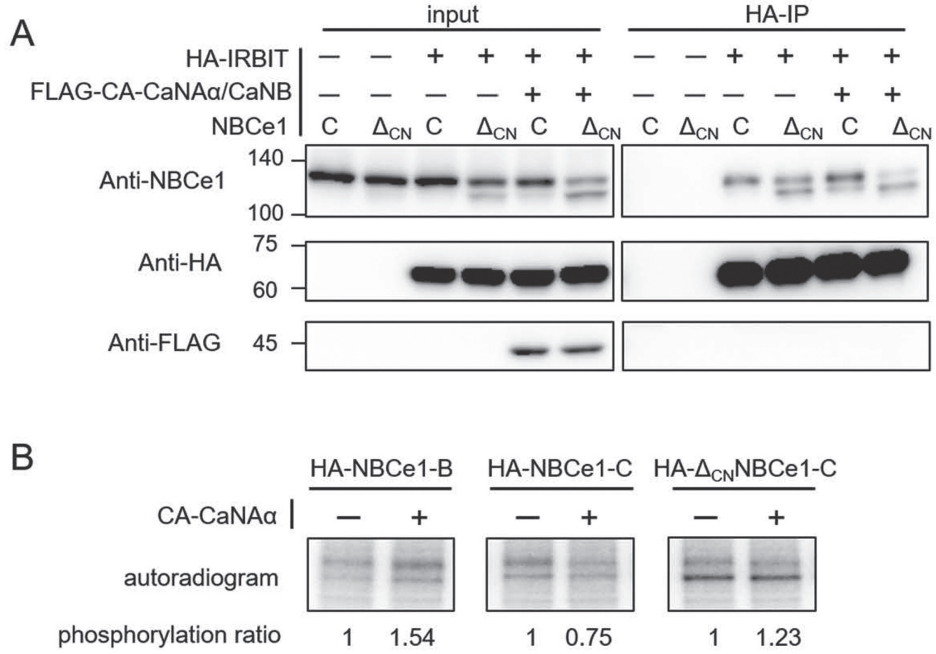

Fig. 6. Effects of Coexpression of CA-CaNAα on the Binding of IRBIT to NBCe1-C and on the Phosphorylation State of NBCe1-C

(A) Effects of coexpression of the CA-CaNAα construct on the interaction between IRBIT and NBCe1-C. HEK293T cells were transfected with the indicated combination of constructs (HA-RIBIT, FLAG-CA-CaNAα, and untagged NBCe1-C), and the interaction between IRBIT and NBCe1-C was examined in a coimmunoprecipitation assay involving the anti-HA antibody. C, NBCe1-C; Δ_{CN}, Δ_{CN}NBCe1-C. **(B)** Effects of coexpression of CA-CaNAα on phosphorylation levels of NBCe1-C were examined. HeLa cells were transfected with each NBCe1-C construct and CA-CaNAα, and were metabolically labeled with [^{32}P]orthophosphate. [^{32}P]labeled NBCe1-C was immunopurified with the anti-HA antibody and was separated by SDS-PAGE. Radioactivity of the corresponding band was measured and was normalized to the amount of immunopurified NBCe1-C that was determined by western blotting of the same sample. *Top*: an autoradiogram of immunopurified NBCe1-C after SDS-PAGE, *lower panel*: the numbers indicate relative phosphorylation levels in each condition (phosphorylation levels of NBCe1-C alone are set to 1.0).

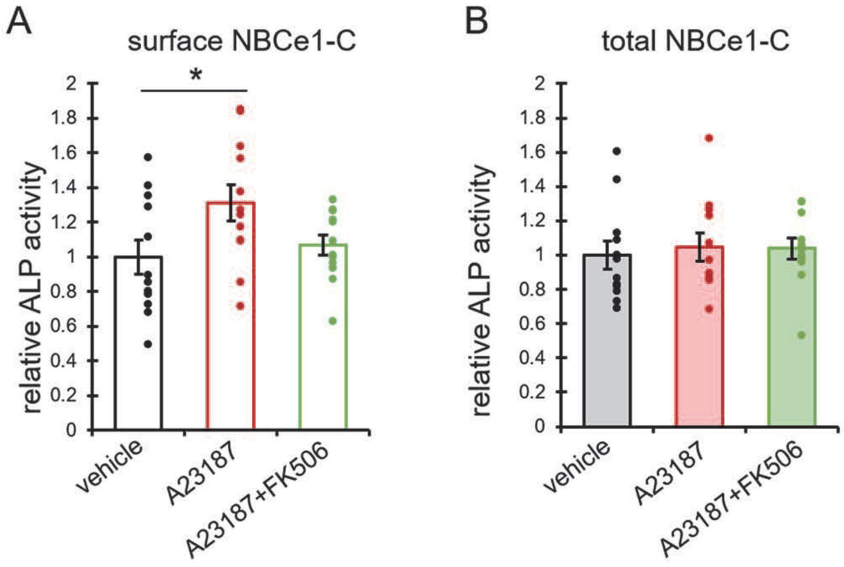

Fig. 7. Surface Expression of NBCe1-C Is Enhanced in Response to Increases in Cytosolic Ca^{2+} Concentration

(A) Effects of intracellular Ca^{2+} concentration increase and a calcineurin inhibitor, FK506, on the surface expression of NBCe1-C stably expressed in HeLa cells. Surface expression levels were quantified by measuring ALP activity of non-permeabilized cells. Vehicle: 0.1% DMSO, A23187: 2 μM A23187, and A23187+FK506: 2 μM A23187 *plus* 10 μM FK506 **(B)** Total expression levels of NBCe1-C were quantified by measuring ALP activity of permeabilized cells. Vehicle: 0.1% DMSO, A23187: 2 μM A23187, and A23187+FK506: 2 μM A23187 *plus* 10 μM FK506. Data were collected from 12 samples from three independent experiments. Error bars represent SEM. One-way ANOVA (surface NBCe1-C, $F = 3.377$, $p < 0.05$; and total NBCe1-C, $F = 0.115$, $p > 0.05$) and Tukey HSD *post hoc* test were carried out; $*p < 0.05$.

in vivo was confirmed, most of functional experiments were conducted with CaNAα constructs.

Calcineurin binds to substrates via two short motifs, PxIxIT and LxVP.[26,27] In the case of NBCe1-C, a PxIxIT-type docking motif, PQIRIE, was found in the unique C-terminal region (Figs. 1 and 2). Some substrates, such as NFAT and TRESK[42,43] have both motifs in their sequences. Neither NBCe1-B nor Δ_{CN}NBCe1-C, a deletion mutant for this motif, manifested any binding to calcineurin, suggesting that PQIRIE is a critical determinant of the interaction between NBCe1-C and calcineurin, as is the case for the interaction between an NBCn1 splice variant and calcineurin.[44]

We showed that the surface expression of NBCe1-C was significantly enhanced by CA-CaNAα coexpression (Fig. 4); however, the surface expression of NBCe1-B and Δ_{CN}NBCe1-C was also enhanced but at a lesser extent (Fig. 4). It is well known that calcineurin is involved in endocytosis of synaptic vesicles,[45,46] and it is reported that surface expression of membrane proteins is regulated by calcineurin not through direct dephosphorylation but through dephosphorylation of the endocytotic machinery or regulation of gene expression.[47–49] Furthermore, the critical involvement of calcineurin in the activation of TFEB and TFE3, the two master regulators of lysosomal biogenesis responses, was recently reported.[50,51] Therefore, we can hypothesize that the enhancement of the surface expression of NBCe1-B or Δ_{CN}NBCe1-C by CA-CaNAα is due to these indirect effects of calcineurin.

We can conclude that calcineurin dephosphorylates NBCe1-C by docking via its PQIRIE motif, resulting in enhancement of the surface expression of NBCe1-C. Although how the dephosphorylation of NBCe1-C by calcineurin is linked to the enhancement of its surface expression remains uncertain, there are two possible mechanisms. First, dephosphorylation by calcineurin may prompt the transport/maturation of NBCe1-C from the endoplasmic reticulum to Golgi apparatus and/or from the Golgi apparatus to cell surface. We noticed that Δ_{CN}NBCe1-C during SDS-PAGE showed upregulation of a faster-migrating moiety representing insufficient glycosylation (see Supplementary Fig. S3), which implied the cause of the lower surface expression. Nevertheless, the extent of the reduction in surface expression was not parallel to the extent of the upregulation of the faster-migrating band, and the migration pattern of wild-type NBCe1-C was not affected after coexpression with CA-CaNAα or incubation with FK506. Therefore, it is not likely that dephosphorylation by calcineurin regulates the glycosylation state of NBCe1-C. Second, dephosphorylation by calcineurin may alter the balance between the endocytosis and degradation of NBCe1-C from the cell surface and its recycling back to the cell surface. The finding that dephosphorylation of NBCe1-C preferentially occurred in the upper maturated NBCe1-C moiety supports this idea (Fig. 6B); however, more direct experiments for revealing the dynamics of NBCe1-C should be conducted.

Due to the limited recovery of the NBCe1-C protein for quantitative phosphoproteomic analysis, we could not identify the sites dephosphorylated by calcineurin. Considering that the PxIxIT binding site of calcineurin is far from its catalytic center (~32 Å)[52,53] and sequences similar to the redefined π-Φ-L-x-[VPL]-[PK] motif[54] were found in the N-terminal cytoplasmic region of NBCe1-C, dephosphorylation sites can be located in the N-terminal region. There are some reports about the regulation of surface expression and/or transport activity associated with phosphorylation of NBCe1-A or -B.[55–58] In these studies, the direction of change in surface expression in response to stimuli depended on experimental conditions, and phosphorylation sites were not determined. Considering the high homology between NBCe1-B and NBCe1-C, the sites dephosphorylated by calcineurin might be involved in the aforementioned findings.

Our observations are almost limited to heterologous expression systems; however, a complex between NBCe1-C and calcineurin certainly exists in the brain. Strong conservation of the PQIRIE calcineurin-docking motif as well as the ETTL PDZ ligand sequence in the C-terminal tail of brain-specific NBCe1-C implies that the regulation of NBCe1-C by calcineurin takes place in the central nervous system. Our future goals are to verify the possibility and to elucidate physiological significance of the regulation of NBCe1-C surface expression by calcineurin in the brain.

Acknowledgments The authors thank Dr. George Seki at Yaizu City Hospital, Yaizu, Japan, for the human NBCe1-B cDNA clone; Dr. Yasuo Watanabe at Showa Pharmaceutical University for mouse cDNAs of constitutively active (CA)-CaNAα and calcineurin B (CaNB) subunits in the pME18S expression vector; Dr. Ichiro Fujimoto for preliminary experiments for this work. This study was supported by Japan Society for the Promotion of Science Grant-in-Aid for Scientific Research C 16K07068 (to A.M.).

Author contributions A.M. and K.M. designed the study; N.H., N.H., S.T., S.K., and A.M. conducted the experiments and analyzed the data; N.H. and A.M. wrote the manuscript. All the authors discussed the results and commented on the manuscript.

Additional Information The online version of this article contains supplementary materials.

Conflict of interest The authors declare no conflict of interest.

REFERENCES

1) Parker MD, Boron WF. The divergence, actions, roles, and relatives of sodium-coupled bicarbonate transporters. *Physiol. Rev.*, **93**, 803–959 (2013).
2) Kurtz I. NBCe1 as a model carrier for understanding the structure-function properties of Na^+ -coupled SLC4 transporters in health and disease. *Pflugers Arch.*, **466**, 1501–1516 (2014).
3) Liu Y, Yang J, Chen LM. Structure and function of SLC4 family HCO_3^- transporters. *Front. Physiol.*, **6**, 355 (2015).
4) Shirakabe K, Priori G, Yamada H, Ando H, Horita S, Fujita T, Fujimoto I, Mizutani A, Seki G, Mikoshiba K. IRBIT, an inositol 1,4,5-trisphosphate receptor-binding protein, specifically binds to and activates pancreas-type Na^+/HCO_3^- cotransporter 1 (pNBC1). *Proc. Natl. Acad. Sci. USA*, **103**, 9542–9547 (2006).
5) Ando H, Kawaai K, Mikoshiba K. IRBIT: a regulator of ion channels and ion transporters. *Biochim. Biophys. Acta*, **1843**, 2195–2204 (2014).
6) Thornell IM, Bevensee MO. Regulators of Slc4 bicarbonate transporter activity. *Front. Physiol.*, **6**, 166 (2015).
7) Bevensee MO, Schmitt BM, Choi I, Romero MF, Boron WF. An electrogenic Na^+-HCO_3^- cotransporter (NBC) with a novel COOH-terminus, cloned from rat brain. *Am. J. Physiol. Cell Physiol.*, **278**, C1200–C1211 (2000).
8) Liu Y, Xu JY, Wang DK, Wang L, Chen LM. Cloning and identification of two novel NBCe1 splice variants from mouse reproductive tract tissues: a comparative study of NCBT genes. *Genomics*, **98**, 112–119 (2011).
9) Igarashi T, Inatomi J, Sekine T, Cha SH, Kanai Y, Kunimi M, Tsukamoto K, Satoh H, Shimadzu M, Tozawa F, Mori T, Shiobara M, Seki G, Endou H. Mutations in SLC4A4 cause permanent isolated proximal renal tubular acidosis with ocular abnormalities. *Nat. Genet.*, **23**, 264–266 (1999).
10) Myers EJ, Marshall A, Parker MD. The role of disease-linked residue glutamine-913 in support of the structure and function of the human electrogenic sodium/bicarbonate cotransporter NBCe1-A. *Sci. Rep.*, **8**, 3066 (2018).
11) Horita S, Simsek E, Simsek T, Yildirim N, Ishiura H, Nakamura M, Satoh N, Suzuki A, Tsukada H, Mizuno T, Seki G, Tsuji S, Nangaku M. SLC4A4 compound heterozygous mutations in exon-intron boundary regions presenting with severe proximal renal tubular acidosis and extrarenal symptoms coexisting with Turner's syndrome: a case report.

BMC Med. Genet., **19**, 103 (2018).
12) Gawenis LR, Bradford EM, Prasad V, Lorenz JN, Simpson JE, Clarke LL, Woo AL, Grisham C, Sanford LP, Doetschman T, Miller ML, Shull GE. Colonic anion secretory defects and metabolic acidosis in mice lacking the NBC1 Na^+/HCO_3^- cotransporter. *J. Biol. Chem.*, **282**, 9042–9052 (2007).
13) Majumdar D, Maunsbach AB, Shacka JJ, Williams JB, Berger UV, Schultz KP, Harkins LE, Boron WF, Roth KA, Bevensee MO. Localization of electrogenic Na/bicarbonate cotransporter NBCe1 variants in rat brain. *Neuroscience*, **155**, 818–832 (2008).
14) Zhang Y, Chen K, Sloan SA, Bennett ML, Scholze AR, O'Keeffe S, Phatnani HP, Guarnieri P, Caneda C, Ruderisch N, Deng S, Liddelow SA, Zhang C, Daneman R, Maniatis T, Barres BA, Wu JQ. An RNA-sequencing transcriptome and splicing database of glia, neurons, and vascular cells of the cerebral cortex. *J. Neurosci.*, **34**, 11929–11947 (2014).
15) Rickmann M, Orlowski B, Heupel K, Roussa E. Distinct expression and subcellular localization patterns of Na^+/HCO_3^- cotransporter (SLC 4A4) variants NBCe1-A and NBCe1-B in mouse brain. *Neuroscience*, **146**, 1220–1231 (2007).
16) Svichar N, Esquenazi S, Chen HY, Chesler M. Preemptive regulation of intracellular pH in hippocampal neurons by a dual mechanism of depolarization-induced alkalinization. *J. Neurosci.*, **31**, 6997–7004 (2011).
17) Deitmer JW, Rose CR. pH regulation and proton signalling by glial cells. *Prog. Neurobiol.*, **48**, 73–103 (1996).
18) Ruminot, I., Schmalzle, J., Leyton, B., Barros, L. F., and Deitmer, J. W. (2017) Tight coupling of astrocyte energy metabolism to synaptic activity revealed by genetically encoded FRET nanosensors in hippocampal tissue. *J Cereb Blood Flow Metab*, 271678X17737012, doi: 10.1177/0271678X17737012.
19) Suzuki M, Van Paesschen W, Stalmans I, Horita S, Yamada H, Bergmans BA, Legius E, Riant F, De Jonghe P, Li Y, Sekine T, Igarashi T, Fujimoto I, Mikoshiba K, Shimadzu M, Shiohara M, Braverman N, Al-Gazali L, Fujita T, Seki G. Defective membrane expression of the Na^+/HCO_3^- cotransporter NBCe1 is associated with familial migraine. *Proc. Natl. Acad. Sci. USA*, **107**, 15963–1596820 (2010).
20) Ando H, Mizutani A, Matsu-ura T, Mikoshiba K. IRBIT, a novel inositol 1,4,5-trisphosphate (IP3) receptor-binding protein, is released from the IP3 receptor upon IP3 binding to the receptor. *J. Biol. Chem.*, **278**, 10602–10612 (2003).
21) Izuchi Y, Takashima T, Hatano N. Rapid and accurate identification of animal species in natural leather goods by liquid chromatography/mass spectrometry. *Mass Spectrom. (Tokyo)*, **5**, A0046 (2016).
22) Ando H, Mizutani A, Kiefer H, Tsuzurugi D, Michikawa T, Mikoshiba K. IRBIT suppresses IP3 receptor activity by competing with IP3 for the common binding site on the IP3 receptor. *Mol. Cell*, **22**, 795–806 (2006).
23) Kanda Y. Investigation of the freely available easy-to-use software 'EZR' for medical statistics. *Bone Marrow Transplant.*, **48**, 452–458 (2013).
24) Kurtz I, Zhu Q. Structure, function, and regulation of the SLC4 NBCe1 transporter and its role in causing proximal renal tubular acidosis. *Curr. Opin. Nephrol. Hypertens.*, **22**, 572–583 (2013).
25) Kuno T, Mukai H, Ito A, Chang CD, Kishima K, Saito N, Tanaka C. Distinct cellular expression of calcineurin A alpha and A beta in rat brain. *J. Neurochem.*, **58**, 1643–1651 (1992).
26) Roy J, Cyert MS. Cracking the phosphatase code: docking interactions determine substrate specificity. *Sci. Signal.*, **2**, re9 (2009).
27) Li H, Rao A, Hogan PG. Interaction of calcineurin with substrates and targeting proteins. *Trends Cell Biol.*, **21**, 91–103 (2011).
28) Nygren PJ, Scott JD. Regulation of the phosphatase PP2B by protein-protein interactions. *Biochem. Soc. Trans.*, **44**, 1313–1319 (2016).
29) Thornell IM, Wu J, Bevensee MO. The IP3 receptor-binding protein IRBIT reduces phosphatidylinositol 4,5-bisphosphate (PIP2) stimulation of Na/bicarbonate cotransporter NBCe1 variants expressed in Xenopus laevis oocytes. *FASEB J.*, **24**, 815.6 (2010).
30) Yang D, Shcheynikov N, Muallem S. IRBIT: it is everywhere. *Neurochem. Res.*, **36**, 1166–1174 (2011).
31) Schmitt BM, Biemesderfer D, Romero MF, Boulpaep EL, Boron WF. Immunolocalization of the electrogenic Na^+-HCO_3^- cotransporter in mammalian and amphibian kidney. *Am. J. Physiol.*, **276**, F27–F38 (1999).
32) Thevenod F, Roussa E, Schmitt BM, Romero MF. Cloning and immunolocalization of a rat pancreatic Na^+ bicarbonate cotransporter. *Biochem. Biophys. Res. Commun.*, **264**, 291–298 (1999).
33) Yang D, Shcheynikov N, Zeng W, Ohana E, So I, Ando H, Mizutani A, Mikoshiba K, Muallem S. IRBIT coordinates epithelial fluid and HCO_3^- secretion by stimulating the transporters pNBC1 and CFTR in the murine pancreatic duct. *J. Clin. Invest.*, **119**, 193–202 (2009).
34) Romero MF, Chen AP, Parker MD, Boron WF. The SLC4 family of bicarbonate (HCO_3^-) transporters. *Mol. Aspects Med.*, **34**, 159–182 (2013).
35) Li HC, Worrell RT, Matthews JB, Husseinzadeh H, Neumeier L, Petrovic S, Conforti L, Soleimani M. Identification of a carboxyl-terminal motif essential for the targeting of Na^+-HCO_3^- cotransporter NBC1 to the basolateral membrane. *J. Biol. Chem.*, **279**, 43190–43197 (2004).
36) Azimov R, Abuladze N, Sassani P, Newman D, Kao L, Liu W, Orozco N, Ruchala P, Pushkin A, Kurtz I. G418-mediated ribosomal read-through of a nonsense mutation causing autosomal recessive proximal renal tubular acidosis. *Am. J. Physiol. Renal Physiol.*, **295**, F633–F641 (2008).
37) Bonifacino JS. Adaptor proteins involved in polarized sorting. *J. Cell Biol.*, **204**, 7–17 (2014).
38) Lasiecka ZM, Winckler B. Mechanisms of polarized membrane trafficking in neurons -- focusing in on endosomes. *Mol. Cell. Neurosci.*, **48**, 278–287 (2011).
39) Bentley M, Banker G. The cellular mechanisms that maintain neuronal polarity. *Nat. Rev. Neurosci.*, **17**, 611–622 (2016).
40) Feng W, Zhang M. Organization and dynamics of PDZ-domain-related supramodules in the postsynaptic density. *Nat. Rev. Neurosci.*, **10**, 87–99 (2009).
41) Zeke A, Lukacs M, Lim WA, Remenyi A. Scaffolds: interaction platforms for cellular signalling circuits. *Trends Cell Biol.*, **19**, 364–374 (2009).
42) Park S, Uesugi M, Verdine GL. A second calcineurin binding site on the NFAT regulatory domain. *Proc. Natl. Acad. Sci. USA*, **97**, 7130–7135 (2000).
43) Czirjak G, Enyedi P. The LQLP calcineurin docking site is a major determinant of the calcium-dependent activation of human TRESK background K^+ channel. *J. Biol. Chem.*, **289**, 29506–29518 (2014).
44) Danielsen AA, Parker MD, Lee S, Boron WF, Aalkjaer C, Boedtkjer E. Splice cassette II of Na^+,HCO_3^- cotransporter NBCn1 (slc4a7) interacts with calcineurin A: implications for transporter activity and intracellular pH control during rat artery contractions. *J. Biol. Chem.*, **288**, 8146–8155 (2013).
45) Cousin MA, Robinson PJ. The dephosphins: dephosphorylation by calcineurin triggers synaptic vesicle endocytosis. *Trends Neurosci.*, **24**, 659–665 (2001).
46) Sun T, Wu XS, Xu J, McNeil BD, Pang ZP, Yang W, Bai L, Qadri S, Molkentin JD, Yue DT, Wu LG. The role of calcium/calmodulin-activated calcineurin in rapid and slow endocytosis at central synapses. *J. Neurosci.*, **30**, 11838–11847 (2010).
47) Gooch JL, Guler RL, Barnes JL, Toro JJ. Loss of calcineurin Aalpha results in altered trafficking of AQP2 and in nephrogenic diabetes insipidus. *J. Cell Sci.*, **119**, 2468–2476 (2006).
48) Bhattacharyya S, Biou V, Xu W, Schluter O, Malenka RC. A critical role for PSD-95/AKAP interactions in endocytosis of synaptic AMPA receptors. *Nat. Neurosci.*, **12**, 172–181 (2009).
49) Fonseca A, Carvalho E, Eriksson JW, Pereira MJ. Calcineurin is an important factor involved in glucose uptake in human adipocytes. *Mol. Cell. Biochem.*, **445**, 157–168 (2018).
50) Medina DL, Di Paola S, Peluso I, Armani A, De Stefani D, Venditti R, Montefusco S, Scotto-Rosato A, Prezioso C, Forrester A, Settembre C, Wang W, Gao Q, Xu H, Sandri M, Rizzuto R, De Matteis MA, Ballabio A. Lysosomal calcium signalling regulates autophagy through calcineurin and TFEB. *Nat. Cell Biol.*, **17**, 288–299 (2015).
51) Raben N, Puertollano R. TFEB and TFE3: linking lysosomes to cellular adaptation to stress. *Annu. Rev. Cell Dev. Biol.*, **32**, 255–278 (2016).
52) Li H, Rao A, Hogan PG. Structural delineation of the calcineurin-

NFAT interaction and its parallels to PP1 targeting interactions. *J. Mol. Biol.*, **342**, 1659–1674 (2004).
53) Grigoriu S, Bond R, Cossio P, Chen JA, Ly N, Hummer G, Page R, Cyert MS, Peti W. The molecular mechanism of substrate engagement and immunosuppressant inhibition of calcineurin. *PLoS Biol.*, **11**, e1001492 (2013).
54) Sheftic SR, Page R, Peti W. Investigating the human Calcineurin Interaction Network using the piLxVP SLiM. *Sci. Rep.*, **6**, 38920 (2016).
55) Gross E, Fedotoff O, Pushkin A, Abuladze N, Newman D, Kurtz I. Phosphorylation-induced modulation of pNBC1 function: distinct roles for the amino- and carboxy-termini. *J. Physiol.*, **549**, 673–682 (2003).
56) Bachmann O, Reichelt D, Tuo B, Manns MP, Seidler U. Carbachol increases Na^+-HCO_3^- cotransport activity in murine colonic crypts in a M3-, Ca^{2+}/calmodulin-, and PKC-dependent manner. *Am. J. Physiol. Gastrointest. Liver Physiol.*, **291**, G650–G657 (2006).
57) Perry C, Baker OJ, Reyland ME, Grichtchenko II. PKCαβγ- and PKCδ-dependent endocytosis of NBCe1-A and NBCe1-B in salivary parotid acinar cells. *Am. J. Physiol. Cell Physiol.*, **297**, C1409–C1423 (2009).
58) Yu H, Riederer B, Stieger N, Boron WF, Shull GE, Manns MP, Seidler UE, Bachmann O. Secretagogue stimulation enhances NBCe1 (electrogenic N^+/HCO_3^- cotransporter) surface expression in murine colonic crypts. *Am. J. Physiol. Gastrointest. Liver Physiol.*, **297**, G1223–G1231 (2009).